Interband magneto-optical studies of resonant polaron coupling in $CdTe/Cd_{1-x}Mn_xTe$ quantum wells

R. J. Nicholas
Clarendon Laboratory, Department of Physics, Oxford University, Parks Road, Oxford OX1 3PU, United Kingdom and Institute for Solid State Physics, University of Tokyo, 7-22-1 Roppongi, Tokyo 106, Japan

S. Sasaki and N. Miura
Institute for Solid State Physics, University of Tokyo, 7-22-1 Roppongi, Tokyo 106, Japan

F. M. Peeters, J. M. Shi, G. Q. Hai, and J. T. Devreese
Physics Department, University of Antwerp, Universiteitsplein 1, B-2610 Antwerp, Belgium

M. J. Lawless
Clarendon Laboratory, Department of Physics, Oxford University, Parks Road, Oxford OX1 3PU, United Kingdom

D. E. Ashenford and B. Lunn
Department of Engineering Design and Manufacture, Hull University, North Humberside, United Kingdom
(Received 1 March 1994)

Magnetoreflectivity measurements of the 1*s* and 2*s* exciton energies in a $CdTe/Cd_{1-x}Mn_xTe$ superlattice have been made in magnetic fields up to 45 T, showing the resonant polaron coupling of electrons to LO phonons. Strong reflectivity features are seen for both the 1*s* and 2*s* excitons, which show a strong field-dependent spin splitting due to the dilute magnetic barriers. At $B_z=0$, the 2*s* exciton feature is observed lying 18 meV above the 1*s* state, and is shifted upward in energy by the magnetic fields. No resonant behavior occurs when the 2*s* state passes through the LO-phonon energy of 21 meV, but at higher fields of around 20 T, the resonances for both spin states ($\sigma^{\pm}$) of the 2*s* exciton broaden and show a strong anticrossing behavior. These experiments are shown to be in excellent agreement with a theoretical treatment which includes the resonant polaron coupling of the electrons alone. Both experiment and theory demonstrate an extremely strong resonant splitting of the 2*s* exciton states of approximately 11 meV, which is over 50% of the LO-phonon energy. The dominance of single-particle polaron coupling is attributed to the relative sizes of the polaron (35 Å) and the exciton (50 Å) radius.

I. INTRODUCTION

Interband magneto-optical absorption was used for the first observation of resonant polaron coupling in solids,[1] in the weakly polar material InSb, but has subsequently only been described in one further report,[2] on the somewhat more polar material GaAs. In this paper we describe the observation of resonant polaron coupling for the excitonic Landau levels in quantum wells in the $CdTe/Cd_{1-x}Mn_xTe$ material system. This system is particularly interesting since both the excitonic binding energy and the polaron coupling constant are very large in comparison to the systems studied previously, and they are further enhanced by the two-dimensional nature of the system.

Resonant polaron coupling for free carriers, which occurs at the condition

$$\hbar\omega_c=\hbar\omega_{\mathrm{LO}}\ , \tag{1}$$

where ω_c is the cyclotron frequency and ω_{LO} is the longitudinal-optic-phonon frequency, is now relatively well understood in both bulk and two-dimensional systems (see Refs. 3–5 for a review). This is mainly through the experimental studies of cyclotron resonance in both bulk GaAs and related two-dimensional GaAs structures, where the Fröhlich coupling constant $\alpha=0.07$. It is now well established that polaron coupling is significantly reduced by the introduction of Fermi statistics in degenerate systems.[6,7] The most polar materials for which the coupling region has been studied in bulk systems have values of $\alpha\sim0.5$,[8,9] with CdTe ($\alpha\sim0.3$) being the most closely studied around the coupling region.[10–12] The most detailed study for a strongly polar two-dimensional system has been performed using InSe layers,[13] where $\alpha\sim0.3$. In this case, the cyclotron resonance was studied through the resonant coupling region, showing resonances arising from both branches of the polaron.

There have been only limited reports of observations of bound carrier polaron effects, with the first studies reported for bulk CdTe (Refs. 10 and 11) and some more recent work on GaAs.[14,15] These occur most strongly for a shallow donor state at the condition

$$E_{(2p+)}-E_{(1s)}=\hbar\omega_{\mathrm{LO}}\ , \tag{2}$$

where $E_{(1s)}$ and $E_{(2p+)}$ are the energy levels of the 1*s* and $2p+$ states of the shallow donor. Experimental studies

of this coupling have been made on bulk CdTe,[11] although the strong reststrahlen absorption and reflection prevented observations being made close to resonance. More recently, work on bulk GaAs (Refs. 14 and 15) has shown a series of couplings, where $E_{(1s)}$ is replaced by the excited states of the shallow donor state associated with the lower Landau level such as $2p^-$, $3d^{-2}$, $4f^{-3}$, etc. A number of experimental and theoretical studies[16–20] have made similar observations for shallow donor impurities in multiple quantum well (MQW) structures and superlattices[21,22] in GaAs, where the coupling is still relatively weak.

In the present study we have used interband magnetoreflectivity to study the $1s$ and $2s$ excitonic energy levels of a $CdTe/Cd_{1-x}Mn_xTe$ superlattice in high magnetic fields ($B_z \leq 42$ T), which are sufficient to cover the possible range of resonant polaron couplings. These measurements are compared with a theoretical treatment based on the phonon coupling to electrons alone, which is found to provide a good description of the experimental results. No evidence is found for a separate coupling to the excitonic states at an equivalent excitonic resonance condition to Eq. (2), when the level separation between the $1s$ and $2s$ levels is equal to $\hbar\omega_{LO}$.

The main subject of interest in $CdTe/Cd_{1-x}Mn_xTe$ superlattices to date has been in the strong magnetic properties induced due to the *sp-d* exchange interactions between the conduction and valence bands and the Mn^{2+} ions (see Ref. 23 for a review). For example, there is some experimental evidence which suggests that the Mn^{2+} exchange is capable of producing a transition to a type-II superlattice band-edge alignment for the σ^+ spin states.[24,25] This effect is less significant in the structures chosen for study here, since the Mn^{2+} content was relatively high ($x = 0.13$), which tends to suppress the large exchange enhancement of the spin splitting due to the presence of a significant amount of antiferromagnetic Mn^{2+}-Mn^{2+} exchange. These structures can thus be considered as relatively conventional MQW structures with type-I confinement potentials.

II. EXPERIMENT

Low-temperature (4.2 K) magneto reflectivity studies were conducted on a $CdTe/Cd_{1-x}Mn_xTe$ superlattice, grown by MBE on InSb[100] substrates,[26] as a function of magnetic field (B_z) up to 42 T, using a long-pulse (~ 10 mS) pulsed magnetic-field system. The magnetic field was applied perpendicular to the superlattice layers. The sample chosen for particular study was a 15-period superlattice, with 70-Å quantum wells of CdTe, and 150-Å barriers of $Cd_{1-x}Mn_xTe$ with a Mn^{2+} content of $x = 0.13$, grown onto a 1000-Å buffer layer of CdTe. The reflectivity signal was measured using a pulsed Xe-arc flashlamp source, with a ~ 500-μS flash duration fired at the peak field, and detected using an image-intensified photodiode array, gated active for 500 μS at peak field. The spectra were detected via separate input and output fiber optic bundles and light guides, and were normalized to the background Xe-arc spectrum. High-quality spectra were recorded in steady-state magnetic fields of up to 15 T, using multiple scan averaging. A typical series of reflectivity spectra is shown in Fig. 1. The zero field spectrum shows two main features, the strongest of which corresponds to the $1s$ heavy-hole (HH) exciton of the first confined state, and the second which corresponds to the light hole (LH). Due to the high reflectivity of the InSb substrate, the reflectivity spectrum corresponds essentially to the absorption spectrum of the MQW structure which is quite strong due to the effective double pass through the superlattice. On application of the magnetic field, the HH $1s$ state shows a very pronounced spin splitting due to the large magnetic modulation of the valence-band barrier heights caused by the exchange interaction with the Mn^{2+} ions, typical of dilute magnetic structures.[23] It should, however, be borne in mind that this splitting is relatively smaller than that found for lower Mn^{2+} content alloy barriers due to the antiferromagnetic exchange, as mentioned above. The LH shows a similar but weaker splitting, with the lower absorption disappearing under the HH feature above $B_z \sim 20$ T.

The main topic of interest in this paper is the behavior of the HH $2s$ states, which are considerably weaker, and can be seen at about 18 meV above the $1s$ state. These are shown more clearly in the set of curves shown in Fig. 2, which were taken in steady-state fields using polarized light. The $2s$ transitions rapidly become stronger at higher fields, as is also shown in the expanded plots of Fig. 3, until the resonant coupling region is reached. The

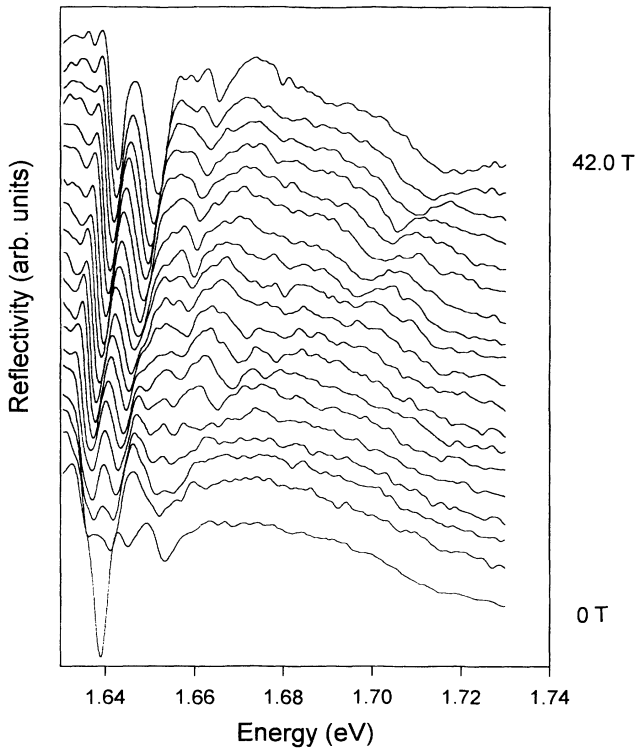

FIG. 1. A series of reflectivity traces as a function of magnetic field from 0 to 42.0 T, taken using unpolarized light. The traces are displaced upward for clarity. The two strongest dips in the zero-field trace correspond to transitions between the highest confined heavy-hole and light-hole states and the lowest confined electron level.

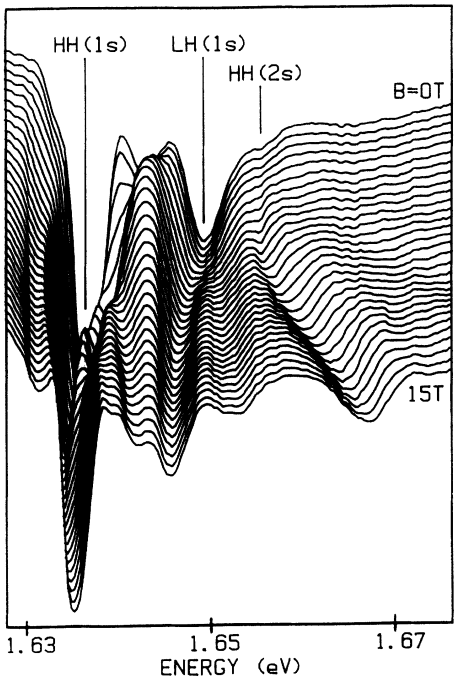

FIG. 2. An expanded low-field (0–15 T) region of the reflectivity, measured using σ^+ polarized light. The strongest dip corresponds to the HH 1*s* exciton, while the HH 2*s* feature is very weak at low fields, but strengthens rapidly above 6 T. Some additional weak features from the opposite spin states are the result of a small amount of σ^- polarized light which is not removed by the low-temperature polarizers.

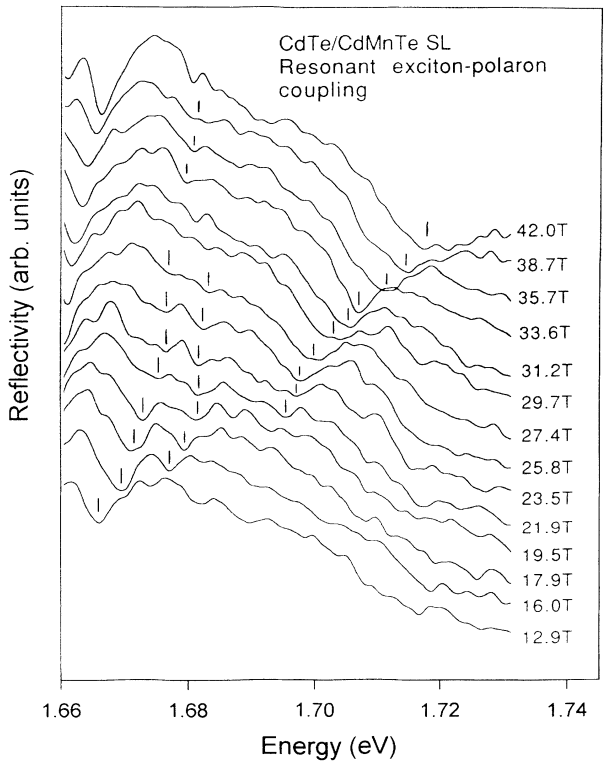

FIG. 3. An expanded section of the high-field reflectivity data in the region of the 2*s* exciton resonant polaron coupling. The field positions assigned to the transitions are indicated.

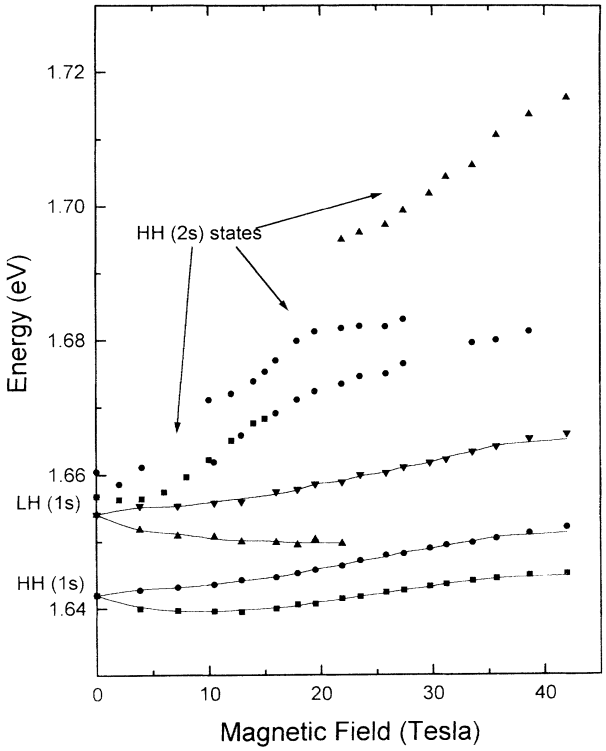

FIG. 4. The transition energies as a function of magnetic field. The 1*s* transition energies are linked by a solid line.

2*s* states then show a very pronounced mixing and anticrossing behavior, with the peaks all but disappearing in the region $B_z = 20$–25 T, and becoming stronger again at higher fields. This behavior can be seen in the plots of transition energies as a function of magnetic field, shown in Fig. 4. In the lower field region the 2*s* states show a similar spin splitting to that found for the 1*s* level, with two peaks clearly seen. By contrast, only one peak is ever resolved in the high-field, high-energy branch. Finally, there is a second broadening of the 2*s* state at fields in the region $B_z \sim 40$ T, and at the same time the transition energy also shows evidence of a second coupling. This is thought to result from a second resonant polaron coupling, corresponding to the coupling to a two optic-phonon state; however, as the data in this region are rather limited, we will confine our further discussion to the main resonant coupling.

III. THEORY

The interpretation of the above results is based on the assumption that the measurement is studying the properties of an excitonic state formed from the interaction of an electron and a hole in a polar material, in which the polaron coupling of the electron (and of the hole if applicable) with the lattice can be treated as the dominant interaction, and the excitonic interaction added as an independent interaction, following the calculation of the electron levels. This approach is suggested by the nature of the observed coupling, which is occurring in the region $B_z \sim 20$ T, where Eq. (1) is known to predict a resonant

interaction for the electrons alone.[11]

The excitonic behavior has been calculated using the memory function approach,[27] to describe the electron polaron coupling, which is then used to describe the deviation from the bare excitonic energy levels. The bare exciton system is modeled by replacing it with a hydrogenlike impurity at the center of a CdTe quantum well with the following material parameters: well width, $L_w=67$ Å; confinement potential $V_0=100$ meV; effective electron mass $m_e^*=0.102m_0$; and the static dielectric constant $\epsilon_0=10.2$. The effective electron mass has been increased over the band-edge value, in order to take account of the nonparabolicity due to the quantum well confinement, using the approach developed by Ekenberg[28] and used successfully to describe the properties of $GaAs/Ga_{1-x}Al_xAs$ quantum wells by Warburton *et al.*[29] The system is then described by the Hamiltonian

$$H_e(\mathbf{r})=-\nabla^2-\gamma\frac{\partial}{\partial\phi}+\tfrac{1}{4}\gamma^2\rho^2-\frac{2}{r}+V(z)\ , \tag{3}$$

with the potential $V(z)$ given as

$$V(z)=\begin{cases}0, & |z|<L_w/2\\ 100\text{ meV}, & |z|>L_w/2\end{cases}, \tag{4}$$

corresponding to the electron confinement potential with a valence-band offset $Q_{vb}=E_{vb}/E_g=0.2$, and we use the following units: (1) length,

$$a_0^*=\hbar^2\epsilon_0/m_e^*e^2=59.12\text{ Å}\ ,$$

(2) energy,

$$R^*=e^2/2\epsilon_0a_0^*=13.34\text{ meV}\ ,$$

and (3) magnetic field,

$$\gamma=e\hbar B/2m_e^*cR^*=0.0425B(T)\ .$$

The Hamiltonian is solved through a variational approach using the following trial functions for the $1s$ state (see Refs. 21 and 15 for details):

$$\Psi_{1s}(\mathbf{r})=f(z)e^{(-\xi_{1s}\rho^2-\eta_{1s}\sqrt{\rho^2+z^2})}\ , \tag{5}$$

and for the $2s$ state,

$$\Psi_{2s}(\mathbf{r})=f(z)e^{(-\xi_{2s}\rho^2-\eta_{2s}\sqrt{\rho^2+z^2})}(1-\lambda\sqrt{\rho^2+\sigma^2z^2})\ , \tag{6}$$

where $f(z)$ is the lowest-energy solution of the quantum well, with

$$E_{z,1}=3.374R^*=45.01\text{ meV}\ ,$$

and λ is determined by the orthogonality condition between the $1s$ and $2s$ states.

The energy levels are then obtained by minimizing

$$E_{1s}^0=\frac{\langle\Psi_{1s}|H_e|\Psi_{1s}\rangle}{\langle\Psi_{1s}|\Psi_{1s}\rangle}\quad\text{and}\quad E_{2s}^0=\frac{\langle\Psi_{2s}|H_e|\Psi_{2s}\rangle}{\langle\Psi_{2s}|\Psi_{2s}\rangle}\ , \tag{7}$$

with respect to ξ_{1s} and η_{1s}, and to ξ_{2s}, η_{2s}, and σ.

The next step is to perform an independent calculation of the free-electron polaron correction. The electron-phonon interaction Hamiltonian

$$H_I=\sum_{\mathbf{q}}(V_{\mathbf{q}}a_{\mathbf{q}}e^{i\mathbf{q}\cdot\mathbf{r}}+V_{\mathbf{q}}^*a_{\mathbf{q}}^\dagger e^{-i\mathbf{q}\cdot\mathbf{r}}) \tag{8}$$

is used, with

$$|V_{\mathbf{q}}|^2=4\pi\alpha(\hbar\omega_{\mathrm{LO}})^{3/2}/q^2\Omega\ ,$$

where $\hbar\omega_{\mathrm{LO}}=21.1$ meV is the LO-phonon energy and $\alpha=0.3$ the electron-phonon coupling constant.

The energy-level separations were calculated from the resonances appearing in the magneto-optical absorption spectrum[27]

$$\frac{-\mathrm{Im}\Sigma(\omega)}{[\omega-\omega_c-\mathrm{Re}\Sigma(\omega)]^2+\mathrm{Im}\Sigma(\omega)]^2}\ , \tag{9}$$

with $\omega_c=eB/m_e^*c$, and $\Sigma(\omega)$ is the memory function which is calculated using second-order perturbation theory and is given by

$$\Sigma(\omega)=\frac{1}{\omega}\int_0^\infty dt(1-e^{i\omega t})\mathrm{Im}F(t)\ . \tag{10}$$

This approach is chosen in the present case since it has the particular advantage of being valid up to higher values of α (Ref. 27). We take zero temperature and incorporate only LO-phonon scattering, and no broadening of the density of states, which implies that $\mathrm{Im}\Sigma(\omega)=0$ As a consequence, the cyclotron resonance frequency is obtained from the solution $\omega=\omega_c^*$ of the following nonlinear equation:

$$\omega-\omega_c-\mathrm{Re}\Sigma(\omega)=0\ . \tag{11}$$

Band nonparabolicity due to the in-plane motion is included through the Kane model[30]

$$E_{np}=\frac{E_g}{2}\left[-1+\left[1+\frac{4E_p}{E_g}\right]^{1/2}\right], \tag{12}$$

where E_p is the energy for a parabolic band, E_{np} the corrected energy due to the nonparabolic band structure, and $E_g=1606$ meV the energy gap of CdTe.

Finally, the transition energy is obtained, first without electron-phonon interaction:

$$E_t^0=E_{2s}^0-E_{1s}^0+\hbar\omega_p^*\ , \tag{13}$$

where $\hbar\omega_p^*$ is the energy difference of the initial states, the first two hole Landau levels, calculated using a hole effective mass of $0.76m_e^*$. The electron-phonon interaction can then be included as

$$E_t=E_t^0+\Delta\hbar\omega_c^*\ , \tag{14}$$

where $\Delta\omega_c^*=\omega_c^*-\omega_c$, with ω_c^* determined by Eq. (13). We can also write this as

$$\Delta\hbar\omega_c^*=\Delta E(N=1)-\Delta E(N=0)\ ,$$

where $E(N)$ is the energy of a free electron in Landau level N and $\Delta E(N)$ the polaron correction to this level. This thus represents the energies of the free-electron transitions corrected by the addition of the excitonic binding energies for the $1s$ and $2s$ states as calculated before the polaron correction was applied.

IV. COMPARISON OF THEORY AND EXPERIMENT

In order to make an accurate comparison with experiment and to eliminate the influence of the spin splitting on the calculations, the splitting of the 1*s* and 2*s* states (the equivalent of the impurity shifted cyclotron resonance energy) is plotted as a function of magnetic field for both experiment and theory in Fig. 5. This illustrates very clearly the dominant effect of the resonant coupling around 20 T, and the excellent agreement between the theory and experiment for a wide range of magnetic fields. Some details of the results require more detailed comment, which we offer below.

(i) There is a significant weakening of the σ^+ transition at higher fields, and only the σ^- transitions are observed for the upper branch. This is attributed to the change in band alignment caused by the lowering of the barrier height for the $m_j = -\frac{3}{2}$ heavy-hole states which, it has been suggested, will lead to the formation of a type-II superlattice alignment at high fields.[24,25] The exact field for this will depend on both the band offset assumed and the Mn^{2+} content of the alloy barriers, but will be counteracted by the Coulomb interaction of the exciton.[25,31,32] There will, however, be a steady lowering of the $m_j = -\frac{3}{2}$ barrier which will produce a significant reduction in the excitonic oscillator strength due to the decreased overlap of the electron and hole wave functions.

(ii) There is an apparently smaller resonant polaron interaction for the σ^- transition, as suggested by the experimental points for the lower branch around 20 T. This may be related to the smaller penetration of the excitonic wave function into the more polar $Cd_{1-x}Mn_xTe$ barriers, although it should also lead to an increased polaron coupling due to the stronger wave-function confinement which leads to a stronger two dimensionality of the excitons.

(iii) The splitting of the upper and lower polaron branches at resonance is ~11 meV, which is over 50% of the energy of the LO phonon (21.3 meV). This is larger than that observed for the branches of the electron cyclotron resonance in the two-dimensional InSe system, and may be attributed to the slightly larger effective Fröhlich coupling constant which is the result partly of the increased quantum well effective mass caused by nonparabolicity of the conduction band.

(iv) No account is taken in the theory of the influence of the polaron mixing of the zeroth and first Landau levels on the excitonic binding energy. This would be a second-order interaction mixing the excitonic and polaron coupling. The most likely effect of this would be an increase in the 2*s* exciton binding energy in the region where the two Landau levels are coupled.

The main conclusion is that we have measured the excitonic polaron coupling in a strongly polar semiconductor superlattice and shown that it can be well described in terms of a theoretical treatment based on a single-particle polaron coupling with electrons alone. The excitonic interaction is then added as a perturbation to the coupled energy levels. Despite the very similar values of the optic-phonon energy and the excitonic Rydberg (both ~21 meV), no evidence was found for any form of composite excitonic polaron coupling, suggesting that the optic-phonon coupling is dominant. This result is rather surprising, in view of the relatively large value of the excitonic binding energy. One possible explanation may lie in the relative sizes of the polaron and excitonic radii, which, are respectively, 35 and 50 Å. Although this difference does not at first sight seem sufficiently large to explain the almost complete absence of excitonic polaron coupling, it may be the case that the ordering of the strengths of the coupling is critical, leading to the possibility of a swap over to excitonic coupling for materials with a higher exciton binding energy.

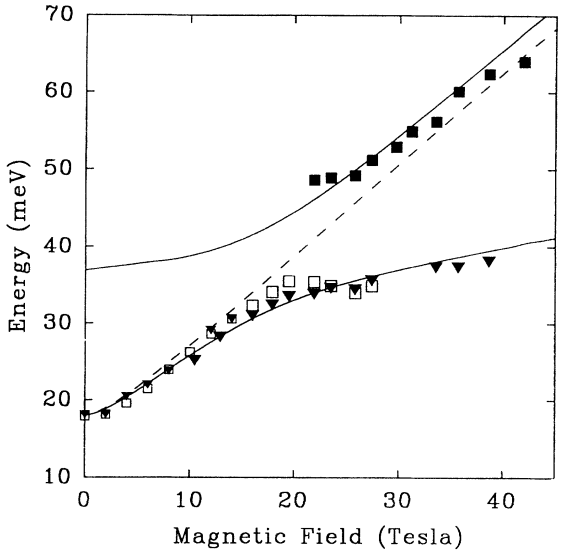

FIG. 5. The experimental splitting of the 1*s*-2*s* exciton transitions for both spin plus ($+\frac{3}{2} - +\frac{1}{2}$, square symbols) and spin minus ($-\frac{3}{2} - -\frac{1}{2}$, triangles). The large and small symbols show data taken using the pulsed and steady fields. The solid line shows the results of the theoretical calculations, including polaron coupling, while the dashed line shows the exciton splitting in the absence of polaron effects.

ACKNOWLEDGMENTS

This work was supported by the "British-Flemish Academic Research Collaboration Programme," the British Council-Monbusho, and S.E.R.C. U.K.

[1]E. J. Johnson and D. M. Larsen, Phys. Rev. Lett. **16**, 655 (1966).

[2]W. Becker, B. Gerlach, T. Hornung and R. G. Ulbrich, in *Proceedings of the International Conference on the Physics of Semiconductors, Stockholm, 1986,* edited by O. Engstrom (World Scientific, Singapore, 1986), p. 1713.

[3]A. Petrou and B. D. McCombe, in *Landau Level Spectroscopy,* edited by G. Landwehr and E. I. Rashba, Modern Problems

in Condensed Matter Sciences Vol. 27.2 (North-Holland, Amsterdam, 1991).

[4]R. J. Nicholas, D. J. Barnes, D. R. Leadley, C. J. G. M. Langerak, J. Singleton, P. J. van der Wel, J. A. A. J. Perenboom, J. J. Harris, and C. T. Foxon, in *Spectroscopy of Semiconductor Microstructures,* Vol. 206 of *NATO Advanced Study Institute, Series B: Physics,* edited by G. Fasol, A. Fasolino, and P. Lugli (Plenum, New York, 1990), p. 451.

[5]R. J. Nicholas, in *Handbook on Semiconductors,* 2nd ed., edited by M. Balkanski (North-Holland, Amsterdam, 1994), Vol. 2.

[6]C. J. G. M. Langerak, J. Singleton, P. J. van der Wel, J. A. Perenboom, D. J. Barnes, R. J. Nicholas, M. A. Hopkins, and C. T. B. Foxon, Phys. Rev. B **38**, 13 133 (1988).

[7]Wu Xiaoguang, F. M. Peeters, and J. T. Devreese, Phys. Rev. B **34**, 8800 (1986).

[8]N. Miura, G. Kodo, and S. Chikazumi, *Proceedings of the International Conference on the Physics of Semiconductors, Edinburgh, 1978,* edited by B. L. H. Wilson, IOP Conf. Ser. No. 43 (Institute of Physics and Physical Society, London, 1979), p. 1109.

[9]Y. Imanaka, N. Miura, and H. Kukimoto, Phys. Rev. B **49**, 16 965 (1994).

[10]D. R. Cohn, D. M. Larsen, and B. Lax, Solid State Commun. **8**, 1707 (1970).

[11]D. R. Cohn, D. M. Larsen, and B. Lax, Phys. Rev. B **6**, 1367 (1972).

[12]F. M. Peeters and J. T. Devreese, Physica B **127**, 408 (1984).

[13]R. J. Nicholas, M. Watts, D. F. Howell, F. M. Peeters, X.-G. Wu, J. T. Devreese, L. van Bockstal, F. Herlach, C. J. G. M. Langerak, J. Singleton, and A. Chevy, Phys. Rev. B **45**, 12 144 (1992).

[14]J. P. Cheng, B. D. McCombe, J. M. Shi, F. M. Peeters, and J. T. Devreese, Phys. Rev. B **48**, 7910 (1993).

[15]J. M. Shi, F. M. Peeters, and J. T. Devreese, Phys. Rev. B **48**, 5202 (1993).

[16]N. C. Jarosik, B. D. McCombe, B. V. Shanabrook, J. Comas, J. Ralston, and G. Wicks, Phys. Rev. Lett. **54**, 1283 (1985).

[17]J. P. Cheng and B. D. McCombe, Phys. Rev. B **42**, 7626 (1990).

[18]Y. H. Chang, B. D. McCombe, J. M. Mercy, and A. A. Reeder, Phys. Rev. Lett. **61**, 1408 (1988).

[19]S. Huant, W. Knap, G. Martinez, and B. Etienne, Europhys. Lett. **7**, 159 (1988).

[20]S. Huant, S. P. Najda, W. Knap, G. Martinez, B. Etienne, C. J. G. M. Langerak, J. Singleton, R. A. J. Thomeer, G. Hai, F. M. Peeters, and J. T. Devreese, in *Proceedings of the 20th International Conference on the Physics of Semiconductors,* edited by E. M. Anastassakis and J. D. Joannopoulos (World Scientific, Singapore, 1990), p. 1369.

[21]J. M. Shi, F. M. Peeters, G. Q. Hai, and J. T. Devreese, Phys. Rev. B **44**, 5692 (1991).

[22]F. M. Peeters, J. M. Shi, J. T. Devreese, J. P Cheng, B. D. McCombe, and W. Schaff, Solid-State Electron. **37**, 1217 (1994).

[23]J. K. Furdyna, J. Appl. Phys. **64**, R29 (1988).

[24]E. Delporte, J. M. Berroir, G. Bastard, C. Delalande, J. M. Hong, and L. L. Chang, Phys. Rev. B **42**, 5891 (1990).

[25]A. A. Wasiela, P. Peyla, Y. Merle d'Aubigne, J. E. Nocholls, D. E. Ashenford, and B. Lunn, Semicond. Sci. Technol. **7**, 571 (1992).

[26]A. A. Wasiela, Y. Merle d'Aubigne, J. E. Nocholls, D. E. Asshenford, and B. Lunn, Solid State Commun. **26**, 263 (1990).

[27]F. M. Peeters, X.-G. Wu, and J. T. Devreese, Phys. Rev. B **34**, 1160 (1986).

[28]U. Ekenberg, Phys. Rev. B **40**, 7714 (1989).

[29]R. J. Warburton, J. G. Michels, R. J. Nicholas, J. J. Harris, and C. T. Foxon, Phys. Rev. B **46**, 13 394 (1992).

[30]E. J. Kane, J. Phys. Chem. Solids **1**, 247 (1957).

[31]R. J. Nicholas, Physica B **191**, 156 (1993).

[32]V. A. Chitta (unpublished).